Pramana – J. Phys. (2017) 89:16
DOI 10.1007/s12043-017-1415-y

Microscopic theory of substrate-induced gap effect on real AFM susceptibility in graphene

SIVABRATA SAHU[1], S K PANDA[2] and G C ROUT[3,*]

[1]School of Applied Sciences (Physics), Campus-3, KIIT University, Bhubaneswar 751 024, India
[2]K.D. Science College, Pochilima, Hinjilicut 761 101, India
[3]Condensed Matter Physics Group, Physics Enclave, Plot No. 664/4825, Lane-4A, Shree Vihar, Chandrasekharpur, Po-Patia, Bhubaneswar 751 031, India
*Corresponding author. E-mail: gcr@iopb.res.in

Published online 24 June 2017

Abstract. We address here a tight-binding model study of frequency-dependent real part of antiferromagnetic susceptibility for the graphene systems. The Hamiltonian consists of electron hopping upto third nearest-neighbours, substrate and impurity effects in the presence of electron–electron interactions at A and B sublattices. To calculate susceptibility, we evaluate the two-particle electron Green's function by using Zubarev's Green's function technique. The frequency-dependent real part of antiferromagnetic susceptibility of the system is computed numerically by taking 1000 × 1000 grid points of the electron momentum. The susceptibility displays a sharp peak at the neutron momentum transfer energy at low energies and another higher energy peak appearing at substrate-induced gap. The evolution of these two peaks is investigated by varying neutron wave vector, Coulomb correlation energy, substrate-induced gap, electron hopping integrals and A- and B-site electron doping concentrations.

Keywords. Graphene; dynamic spin antiferromagnetic susceptibility; Coulomb interaction.

PACS Nos 73.22.Pr; 75.30.cr

1. Introduction

Graphene is a two-dimensional zero-gap semiconductor having honey-comb lattice with one electron per orbital has a half-filled band. The origin of magnetism in graphene is still unclear. The materials with bipartite structure like graphene can exhibit magnetic ordering, which has potential applications in spintronic devices [1]. The repulsive electron–electron interaction in graphene-on-substrate can produce further imbalances in the sublattice atoms leading to spin polarization where the spins of electrons of different sublattice atoms are coupled antiferromagnetically. Many field theoretical calculations [2–4] have predicted defect-induced magnetism in graphene. Recent field theoretical calculation predicts a transition from semimetal to Neel's state in graphene. Sahu *et al* [5] have reported Coulomb interaction effects on band-gap opening in graphene. We consider here the impurity effect on both sublattices of graphene. The polarized substrate-induced gap may further induce spin polarization in the system. In the tight-binding model calculation, we introduce electron–electron interaction in A and B sublattices of graphene in the form of Hubbard model. We calculate the frequency-dependent antiferromagnetic spin susceptibility, which is a two-particle Green's function, by Zubarev's Green's technique. The real part of the susceptibility is computed numerically for 1000 × 1000 grid points of the electron momentum. We report here a tight-binding model study of graphene-on-substrate with impurity and calculate the antiferromagnetic susceptibility.

2. Model Hamiltonian

The tight-binding model Hamiltonian for the monolayer is written as

$$H_1 = \sum_{i,\sigma} \left(\epsilon_a a^{\dagger}_{i,\sigma} a_{i,\sigma} + \epsilon_b\, b^{\dagger}_{i,\sigma} b_{i,\sigma}\right), \tag{1}$$

$$H_2 = \sum_{i,j,\sigma} V\left(x_a\, a^{\dagger}_{i,\sigma} a_{j,\sigma} + x_b\, b^{\dagger}_{i,\sigma} b_{j,\sigma}\right), \tag{2}$$

$$H_3 = \sum_{i,\sigma} \Delta\left(a^{\dagger}_{i,\sigma} a_{i,\sigma} - b^{\dagger}_{i,\sigma} b_{i,\sigma}\right), \tag{3}$$

$$H_4 = -\sum_{\beta=1-3} \sum_{i,j,\sigma} t_\beta \left(a^{\dagger}_{i,\sigma}\, b_{j,\sigma} + b^{\dagger}_{j,\sigma} a_{i,\sigma}\right). \tag{4}$$

Here H_1 represents the on-site hopping of electrons with site energies ϵ_a and ϵ_b at A and B sites, respectively. The Hamiltonian H_2 represents the external doping effect with doping concentrations x_a and x_b respectively at A and B sublattices with same impurity potential V. The Hamiltonian H_3 represents the effect of substrate on graphene which raises the A-site energy by Δ and lowers the B site energy by $-\Delta$, thereby introducing a substrate-induced gap 2Δ. The Hamiltonian H_4 represents the electron hopping upto the third nearest-neighbours represented by $\beta = 1, 2, 3$ and the corresponding electron dispersions are $\epsilon_1(k) = -t_1\gamma_1(k)$, $\epsilon_2(k) = -t_2\gamma_2(k)$ and $\epsilon_3(k) = -t_3\gamma_3(k)$ respectively. The nearest-neighbour complex dispersion $\gamma_1(k)$ is written as

$$\gamma_1(k) = \mathrm{e}^{\left(k_x a/\sqrt{3}\right)} + 2\mathrm{e}^{-(k_x a/2\sqrt{3})} \cos\left(\frac{k_y a}{2}\right). \tag{5}$$

Here t_β and $\gamma_\beta(k)$ with $\beta = 1, 2, 3$ represent the hopping integrals and band dispersions respectively upto third nearest-neighbours. The Hubbard-type electron–electron interaction is introduced as $H_u = U \sum_{\alpha,i} n^{\alpha}_{i,\uparrow} n^{\alpha}_{i,\downarrow}$, where α = A and B sites. The Coulomb interaction is treated here within Hartree–Fock approximation, where the mean occupancies $\langle n^{\alpha}_{-\sigma}\rangle$ of electron at A and B sites for up- and down-spins are computed numerically and self-consistently. The total Hamiltonian induces antiferromagnetism in graphene system.

3. Calculation of dynamic longitudinal susceptibility

The longitudinal antiferromagnetic susceptibility $\chi^{zz}(q, \omega)$ along z-direction is written as

$$\chi^{zz}(q, \omega) = \langle\langle m^z(q, t); m^z(-q, 0)\rangle\rangle_\omega, \tag{6}$$

where the z-component of magnetization due to spins at A and B site electrons is written as $m^z = m_A(q, t) + m_B(q, t)$ where

$$m_A(q, t) = \sum_k \left(a^{\dagger}_{k+q,\uparrow} a_{k,\uparrow} - a^{\dagger}_{k+q,\downarrow} a_{k,\downarrow}\right) \tag{7}$$

$$m_B(q, t) = \sum_k \left(b^{\dagger}_{k+q,\uparrow} b_{k,\uparrow} - b^{\dagger}_{k+q,\downarrow} b_{k,\downarrow}\right). \tag{8}$$

The susceptibility defined in eq. (6) is rewritten in terms of two particle functions as

$$\chi^{zz}(q, \omega) = \sum_{k,\sigma} \sum_{k',q',\sigma'} \sigma\sigma'[\chi_1 - \chi_2 - \chi_3 + \chi_4], \tag{9}$$

where σ and σ' are $+1$ (-1) corresponding to up (down) spin orientations of the electrons and the two-particle Green's functions are written as $\chi_1 = \langle\langle\theta_1; \delta_1\rangle\rangle_\omega$, $\chi_2 = \langle\langle\theta_2; \delta_1\rangle\rangle_\omega$, $\chi_3 = \langle\langle\theta_1; \delta_2\rangle\rangle_\omega$ and $\chi_4 = \langle\langle\theta_2; \delta_2\rangle\rangle_\omega$, where $\theta_1 = a^{\dagger}_{k+q,\sigma} a_{k,\sigma}$, $\theta_2 = b^{\dagger}_{k+q,\sigma} b_{k,\sigma}$, $\delta_1 = a^{\dagger}_{k'-q',\sigma'} a_{k',\sigma'}$ and $\delta_2 = b^{\dagger}_{k'-q',\sigma'} b_{k',\sigma'}$. The above two-particle Green's functions χ_i $(i = 1$ to $4)$ are calculated using Zubarev's technique [6]. During the calculation for each Green's function, we solve the four-coupled Green's function equations. Finally, the frequency-dependent susceptibility is calculated in terms of the Fermi–Dirac distribution functions.

4. Results and discussions

The real part of the dynamic antiferromagnetic spin susceptibility given in eq. (9) is computed to investigate the effect of Coulomb correlation effects, substrate-induced gap, impurity effect and different hopping integral effects. The physical parameters involved in the calculation are made dimensionless with respect to nearest-neighbour hopping integral t_1. The parameters are $\tilde{t}_1 = -1$, $\tilde{t}_2 = t_2/t_1$, $\tilde{t}_3 = t_3/t_1$, impurity potential $v = V/t_1$, Coulomb potential $u = U/t_1$, temperature $t = k_B T/t_1$, applied external frequency $c_1 = \omega/t_1$ and substrate induced gap $d1 = \Delta/t_1$, neutron momentum transfer energy $q_1 = q v_F/t_1$, where v_F and q are respectively the velocity of electrons at Fermi level and neutron momentum. When a neutron beam of frequency ω and momentum q enters into the graphene systems, the neutron beam is absorbed at different energies signifying the energy scales. In the present report, we investigate the frequency-dependent real part of the susceptibility Re. $\chi(q_1, c_1)$ arising due to antiferromagnetically ordered spins of the electrons as shown in figures 1–6.

Figure 1 shows the effect of neutron momentum transfer energy on Re. $\chi(q_1, c_1)$. For $q_1 = 0.01$, we observe a low-energy neutron resonance peak p_1 with height which is nearly 200 times greater than that of the real part Re. $\chi(q_1, c_1)$ reported for the ferromagnetic order case [7]. By increasing q_1, this resonance peak shifts to higher energies. We observe another step function p_2 in the real part of susceptibility Re. $\chi(q_1, c_1)$ arising due to the substrate-induced gap in graphene-on-substrate. The energy corresponding to the mid-point of the step gives rise to substrate-induced gap energy d_1. This gap

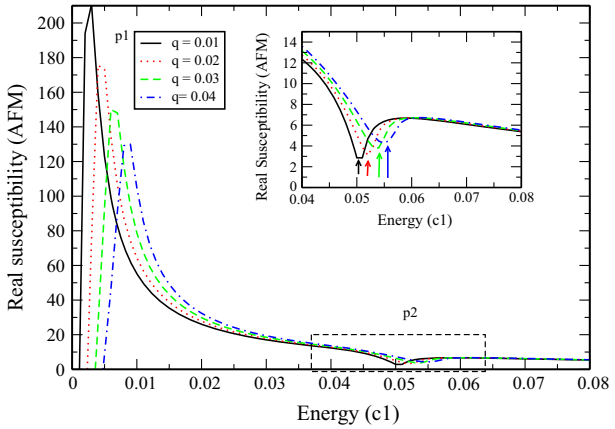

Figure 1. The plot of real susceptibility (AFM) vs. energy (c_1) for different values of neutron momentum transfer energy q_1 on substrate-induced gap $d_1 = 0.04$ for Coulomb potential $u = 2.2$, damping factor $e_1 = 0.001$ at temperature $t = 0.025$.

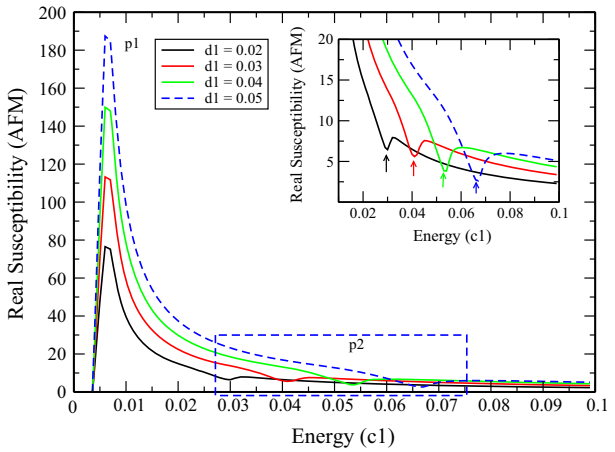

Figure 2. The plot of real susceptibility (AFM) vs. energy (c_1) for different substrate-induced gaps $d_1 = 0.02$, 0.03, 0.04, 0.05, fixed Coulomb potential $u = 2.2$, damping factor $e_1 = 0.001$ and temperature $t = 0.025$ for neutron momentum transfer energy $q_1 = 0.03$.

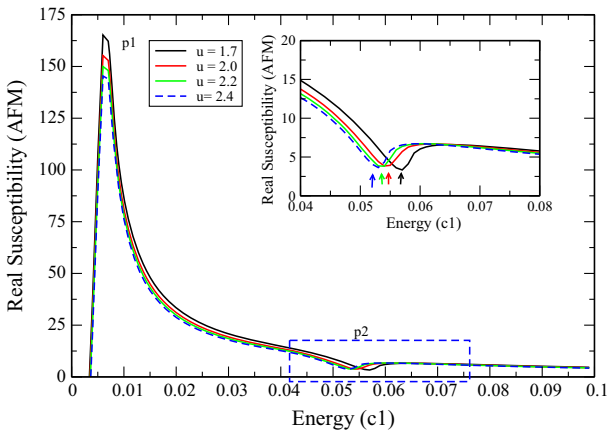

Figure 3. The plot of real susceptibility (AFM) vs. energy (c_1) for different Coulomb potential $u = 1.7, 2.0, 2.2, 2.4$, 2.5, fixed substrate-induced gap $d_1 = 0.04$ at temperature $t = 0.025$ for neutron momentum transfer energy $q_1 = 0.03$.

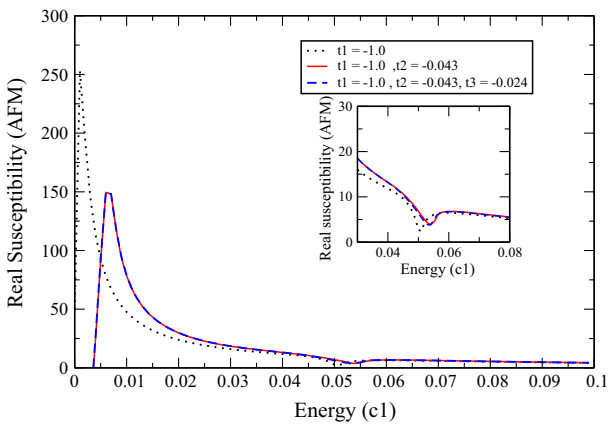

Figure 4. The plot of real susceptibility (AFM) vs. energy (c_1) for different electron hopping $t_1 = -1, t_1 = -1$, $t_2 = -0.043$ and $t_1 = -1, t_2 = -0.043, t_3 = -0.024$, Coulomb potential $u = 2.2$, fixed temperature $t = 0.025$ and substrate-induced gap $d_1 = 0.04$ for neutron momentum transfer energy $q_1 = 0.03$.

shifts to higher energies with increase of q_1 as shown in the inset of figure 1.

Figure 2 shows the plot of frequency-dependent real part of susceptibility Re. $\chi(q_1, c_1)$ for different values of substrate-induced gap $d_1 = 0.02$–0.05. With increase of substrate-induced gap, the position of the resonance peak p_1 corresponding to $q_1 = 0.03$ remains unaltered, while the peak height is suppressed considerably. The step function p_2 shifts to higher energies with increase in substrate-induced gap as shown clearly in the inset of figure 2. It is observed experimentally that the substrate-induced gaps are 250 meV for graphene on substrate SiC [8] and 100 meV for BN system [9].

Figure 3 shows the effect of Coulomb correlation energies $u = 1.7$–2.4 on the frequency-dependent Re. $\chi(q_1, c_1)$. The Coulomb energy does not change position of resonance peak p_1, but suppresses its peak height. The increase of Coulomb energy shifts the step function p_2 to lower energies indicating that the electron–electron correlation suppresses the substrate-induced gap d_1 as shown clearly in the inset of figure 3.

Figure 4 shows the effects of different electron hopping integrals on frequency-dependent Re. $\chi(q_1, c_1)$. The resonance peak p_1 occurs at lower energies for nearest-neighbour hopping $t_1 = -1$. By including second and third nearest-neighbour hoppings, the peak p_1 shifts to higher energies with decrease in its peak height. However, the inclusion of higher-order hopping integrals shifts the step function p_2 to higher energies indicating that it enhances the substrate-induced

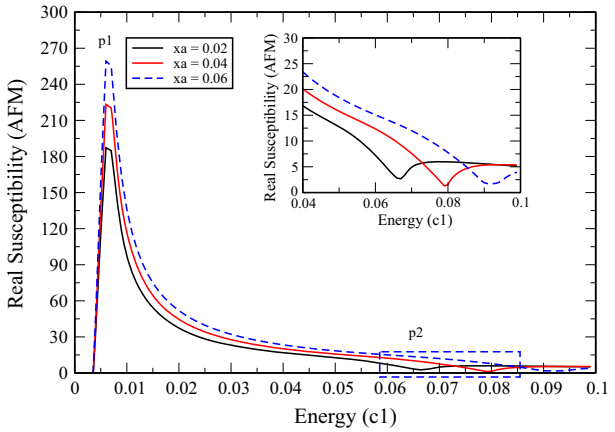

Figure 5. The plot of real susceptibility (AFM) vs. energy (c_1) for different doping concentrations at A site $x_a = 0.02, 0.04, 0.06$ for impurity potential $v = 1$, Coulomb potential $u = 2.2$, damping factor $e_1 = 0.001$ and substrate-induced gap $d_1 = 0.04$ for neutron momentum transfer energy $q_1 = 0.03$.

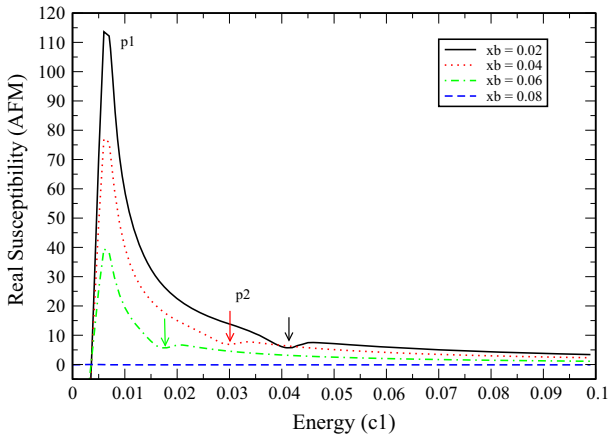

Figure 6. The plot of real susceptibility (AFM) vs. energy (c_1) for different doping concentrations at B site $x_b = 0.02, 0.04, 0.06, 0.08$ for impurity potential $v = 1$, Coulomb potential $u = 2.2$, temperature $t = 0.025$, damping factor $e_1 = 0.001$ and substrate-induced gap $d_1 = 0.04$ for neutron momentum transfer energy $q_1 = 0.03$.

gap. Further, second and third nearest-neighbour hoppings have the same contribution to the step function. Hence, third-nearest-neighbour interaction may be removed from the Hamiltonian having negligible contribution.

Figure 5 shows the effect of A-site electron doping (x_a) on frequency-dependent Re. $\chi(q_1, c_1)$. The increase of electron doping does not change the position of the peak p_1, but enhances its peak height. However, the increase of A-site impurity shifts the step function p_2 to higher energies (see the inset of figure 5). This indicates that A-site impurity enhances the substrate-induced gap.

Figure 6 shows that the effect of B-site electron doping (x_b) on frequency-dependent Re. $\chi(q_1, c_1)$. With increase of B-site doping, the position of the resonance peak p_1 remains unchanged, while its peak height is suppressed considerably and finally vanishes completely for $x_b = 0.08$. The increase of B-site electron doping shifts the step function p_2 towards low energies and finally destroys it. This indicates that the B-site electron doping suppresses the substrate-induced gap and finally destroys the substrate-induced gap for higher doping, i.e. for $x_b = 0.08$.

5. Conclusions

In conclusion, the Coulomb interaction in graphene suppresses the substrate-induced gap. The substrate-induced gap appears in the Re. $\chi(q_1, c_1)$ in the form of a step function which shifts to higher energies with increase of gap magnitude. The first and second nearest-neighbour hoppings are sufficient to describe the kinetic energy effects of electrons in graphene. It is observed that A-site electron doping enhances the substrate-induced gap in graphene, while B-site electron doping suppresses it and even destroys it completely.

Acknowledgements

The authors gracefully acknowledge the research facilities offered by the Institute of Physics, Bhubaneswar, India. The author (Sivabrata Sahu) also acknowledges the leave granted by the authorities of Synergy Institute of Engineering and Technology, Dhenkanal, Odisha to continue the research work.

References

[1] Y W Son *et al*, *Nature* **444**, 347 (2006)
[2] A C Neto, V Kotov, J Nilson, V Pereira and N Peres, *Solid. State Commun*. **149**, 1094 (2009)
[3] O V Yazyer, *Phys. Rev. Lett*. **101**, 037203 (2008)
[4] B Uchoa *et al*, *Phys. Rev. Lett.* **101**, 026805 (2008)
[5] S Sahu and G C Rout, *Physica B* **461**, 49 (2015)
[6] D N Zubarev, *Sov. Phys. Usp*. **3**, 320 (1960)
[7] S Sahu and G C Rout, *Physica B* (2017) (in press)
[8] S Y Zhou *et al*, *Nat. Mater*. **6**, 770 (2007)
[9] G Giovannetti *et al*, *Phys. Rev. B* **76**, 073103 (2007)